



Published in final edited form as:

*Colloids Surf B Biointerfaces*. 2018 June 01; 166: 179–186. doi:10.1016/j.colsurfb.2018.03.019.

## Antibacterial Activity on Superhydrophobic Titania Nanotube Arrays

Kevin Bartlet<sup>1</sup>, Sanli Movafaghi<sup>1</sup>, Lakshmi Prasad Dasi<sup>2</sup>, Arun K. Kota<sup>1,3,4</sup>, and Ketul C. Papat<sup>1,4,\*</sup>

<sup>1</sup>Department of Mechanical Engineering, Colorado State University, Campus Delivery 1374, Fort Collins, CO 80523, USA

<sup>2</sup>Department of Biomedical Engineering, The Ohio State University, Dorothy Davis Heart and Lung Research Institute, Columbus OH 43210, USA

<sup>3</sup>Department of Chemical Engineering, Colorado State University, Campus Delivery 1370, Fort Collins, CO 80523, USA

<sup>4</sup>School of Biomedical Engineering, Colorado State University Campus Delivery 1376, Fort Collins, CO 80523, USA

### Abstract

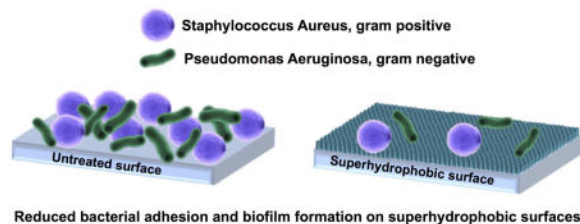
Bacterial infections are a serious issue for many implanted medical devices. Infections occur when bacteria colonize the surface of an implant and form a biofilm, a barrier which protects the bacterial colony from antibiotic treatments. Further, the anti-bacterial treatments must also be tailored to the specific bacteria that is causing the infection. The inherent protection of bacteria in the biofilm, differences in bacteria species (gram-positive vs. gram-negative), and the rise of antibiotic-resistant strains of bacteria makes device-acquired infections difficult to treat. Recent research has focused on reducing biofilm formation on medical devices by modifying implant surfaces. Proposed methods have included antibacterial surface coatings, release of antibacterial drugs from surfaces, and materials which promote the adhesion of non-pathogenic bacteria. However, no approach has proven successful in repelling both gram-positive and gram-negative bacteria. In this study, we have evaluated the ability of superhydrophobic surfaces to reduce bacteria adhesion regardless of whether the bacteria are gram-positive or gram-negative. Although superhydrophobic surfaces did not repel bacteria completely, they had minimal bacteria attached after 24 h and more importantly no biofilm formation was observed.

### Graphical abstract

---

\* Author of correspondence: Ketul C. Papat, ketul.papat@colostate.edu.

**Publisher's Disclaimer:** This is a PDF file of an unedited manuscript that has been accepted for publication. As a service to our customers we are providing this early version of the manuscript. The manuscript will undergo copyediting, typesetting, and review of the resulting proof before it is published in its final citable form. Please note that during the production process errors may be discovered which could affect the content, and all legal disclaimers that apply to the journal pertain.



## Keywords

Superhydrophobic surfaces; bacterial infection; biofilm formation; anti-bacterial surfaces

## 1. Introduction

Bacterial infections are a serious issue for many implanted medical devices. Infections of mechanical heart valves, pacemakers, heart assist devices, etc. are associated with high rates of patient mortality.[1,2] It is estimated that more than half of the hospital-acquired infections in the United States come from biofilms. Biofilms are protective films composed primarily of proteins and polysaccharides created by the bacteria.[3,4] The biofilm protects the bacteria by blocking antibiotics, making these infections difficult to combat.[5–10] Additionally, the overuse of antibiotics is also giving rise to bacteria strains which are resistant to common drugs.[6,9] Infectious bacteria are commonly divided into two categories based on the composition of their cell walls: gram-positive and gram-negative. [5,9–12] Gram-positive bacteria have a cell wall with a layer of peptidoglycan that is typically 15–80 nm thick.[12] The peptidoglycan layer in the cell wall of a gram-negative bacterium is typically 1–2 nm.[12] Common gram-negative bacteria include *Escherichia coli* and *Pseudomonas aeruginosa*, the latter of which is often studied because of its association with device-related infections.[6] *Staphylococcus aureus* is a grampositive bacteria that is found naturally on human skin, and is also commonly associated with device-related infections.[3,13,14] Because these different types of bacteria must be treated with different medications, recent work has focused on modifying the surfaces of implantable medical devices that can reduce adhesion of both gram-positive and gram-negative bacteria.[1]

Different methods of surface modification have been investigated for their potential to reduce medical device-associated infections. A common approach is to modify the surface with antibacterial coatings.[1,15] Other approaches have involved doping materials with silver ions. Silver has been shown to have antibacterial properties, but these surfaces have the same limitations as other antibacterial coatings because the silver ions will eventually diffuse out.[5] Some studies have also looked into using photocatalytic materials that have antibacterial properties when exposed to UV light, but these materials have poor long-term affinities towards organic molecules.[10,11,16] Another approach has been to promote the adhesion of nonpathogenic bacteria over more pathogenic bacteria, but there have been few successes with this approach.[1] To avoid the issues of these approaches, recent studies have looked for ways to prevent the initial attachment of bacteria. One such approach is to employ superhydrophobic surfaces, which display a contact angle greater than 150° and roll-off angle (i.e., the minimum tilt angle of the surface at which liquid droplets starts to roll off

from the surface) less than  $10^\circ$  for water. These differ from superhydrophilic surfaces, which are those that display very low (typically  $<10^\circ$ ) contact angles.

Superhydrophobic surfaces are being investigated for their anti-biofouling properties because the low solid surface energies of these surfaces reduce the adhesion of contaminants and water, making them easy to clean.[17–20] These surfaces are typically fabricated either by covalently attaching molecules with low surface energies to a roughened surface or by roughening the surface of a material which is already hydrophobic.[7,17,21,22] Such surfaces are of interest for a diverse array of applications. For example, superhydrophobic surfaces have been used to reduce the attachment of marine organisms to ship hulls and reduce the drag forces within pipes.[23] They have also been used to create stain-resistant fabrics.[23] As another example, superhydrophobic surfaces have been used to create miniaturized labs for performing biological tests.[24–26] They have also been used to improve the efficiency of turbines and steam engines by reducing the buildup of water.[23] Some previous reports show that superhydrophobic surfaces tend to reduce the attachment of a range of bacteria strains, but other reports show attachment and biofilm formation, indicating that more investigation is needed.[5,9,18,27–30] Further, superhydrophobic surfaces exhibit reduced protein adsorption and any proteins that do adhere are easy to remove.[11,31] These properties are expected to make it more difficult for bacteria to attach and form biofilms on superhydrophobic surfaces.

In this study, we have investigated the adhesion of *S. aureus* and *P. aeruginosa* to superhydrophobic and superhydrophilic titania nanotube arrays. Titanium was chosen as a base material due to its common use in many implantable medical devices. The different surfaces were fabricated by first anodizing and chemically etching titanium to form titania nanotube arrays. The titania nanotube arrays were then silanized to modify the surface chemistry and induce superhydrophobicity or superhydrophilicity. The surfaces were characterized using scanning electron microscopy (SEM) to determine surface topography, contact angle goniometry to determine surface wettability, X-ray photoelectron spectroscopy (XPS) to characterize surface chemistry, and X-ray diffraction (XRD) to examine the crystal structures. *S. aureus* and *P. aeruginosa* adhesion to different surfaces was measured using fluorescence microscopy and SEM, after 6 h and 24 h of culture. The results showed that fewer bacteria attached to the superhydrophobic surfaces when compared to the superhydrophilic and control surfaces. Further, the superhydrophilic surfaces did not show significant differences in the number of attached bacteria when compared to the unmodified titania nanotube arrays.

## 2. Materials and Methods

### 2.1 Fabrication of Titania Nanotube Arrays

Titania nanotube arrays were fabricated from titanium sheets (0.1 cm thick) cut into  $2.5 \times 2.5$  cm squares. The titania nanotube arrays were fabricated using the anodization process described elsewhere.[32–36] The titanium sheet was used as the anode and platinum foil was used as the cathode. The electrolyte used for anodization was composed of 95% v/v diethylene glycol (DEG, Alfa) and 2% v/v hydrofluoric acid (HF, Alfa) by volume in de-ionized (DI) water. The anodization was done for 24 h at 60 V. After anodization, the titania

nanotube arrays were rinsed three times with DI water, dried with nitrogen gas, and annealed for 3 h at 530°C.

Superhydrophobic titania nanotube arrays were fabricated by modifying surfaces with chemical vapor deposition of (heptadecafluoro-1,1,2,2-tetrahydrodecyl)trichlorosilane (referred to as S1 in this manuscript, Gelest). The titania nanotube arrays were first etched with plasma at 200 V in 10 cm<sup>3</sup>/min of oxygen gas for 10 mins and then heated for 1 h at 120°C with 150 µl of S1 in a closed chamber. The superhydrophobic titania nanotube arrays were then rinsed with DI water, dried, and stored until further use.

Superhydrophilic titania nanotube arrays were fabricated by modifying surfaces with polyethylene glycol 2-[methoxy(polyethyleneoxy)propyl]trimethoxysilane (referred to as S2, Gelest). As with the superhydrophobic arrays, the titania nanotube arrays were first etched with plasma at 200 V in 10 cm<sup>3</sup>/min of oxygen gas for 10 mins and then were placed in a 2 vol% of S2 in ethanol solution for 24 h.[37] The superhydrophilic titania nanotube arrays were then rinsed with DI water, dried, and stored until further use.

In this manuscript, the different surfaces are labeled as following: unmodified titanium, referred to as Ti; unmodified titania nanotube arrays, referred to as NT; superhydrophobic titania nanotube arrays, referred to NT-S1; and superhydrophilic titania nanotube arrays, referred to as NT-S2. The surfaces were sterilized in ethanol for 30 mins, then rinsed with DI and dried before all biological experiments.

## 2.2 Surface Characterization

The surface morphology of the titania nanotube arrays was characterized using a JEOL JSM-6500 field emission scanning electron microscope (SEM). The surfaces were coated with 10 nm of gold and imaged at 15 kV. The outer diameters and thicknesses of the nanotubes were measured using ImageJ.

The surface wettability of the different surfaces was characterized using the sessile water droplet method for measuring contact angles. The measurements were taken using a Ramé-Hart Model 250 goniometer connected to a camera. Approximately 10 µl water droplet was formed on a syringe and placed on the substrate surface. Water was added and removed from the droplet to measure the static, advancing and receding contact angles on the surface. Roll-off angles were measured by placing the droplet onto the surface and then tilting the goniometer. Images of the static contact angles were taken after the water droplet had been in contact with the surface for 10 secs. Further, the solid surface energy was estimated using Owens-Wendt analysis (using a surface tension for water of 72.1 mN/m).[37,39]

The surface chemistry of the titania nanotube arrays was characterized using X-ray photoelectron spectroscopy (XPS). Survey spectra were collected along with high resolution spectra scans for titanium and oxygen. The survey spectra were conducted with a pass energy of 187.85 eV from 0 to 1100 eV, while the high-resolution spectra were obtained at a pass energy of 10 eV. The scans were completed using an ESCA Systems X-ray Photoelectron Spectrometer 5800 with a monochromatic Al-K $\alpha$ -X-ray spot source at 1486.6 eV.[38]

The crystal structure of titania nanotube arrays was characterized using X-ray diffraction (XRD). The scans were collected over a  $2\theta$  range of  $20^\circ$  to  $80^\circ$  with  $\theta=1.5^\circ$ . [31] They were run at a rate of 1 step per sec with a step size of  $0.01^\circ$ . DIFFRACT.EVA was used to filter the data and identify the relevant peaks.

### 2.3 Preparation of Bacteria Cultures

*P. aeruginosa* and *S. aureus* cultures were obtained from 10 ml tubes from bacteria solutions stored in glycerol (30% v/v, Sigma) at a concentration of 15% v/v and stored in a  $-80^\circ\text{C}$  freezer. The culture preparation steps are described elsewhere. [6] Prior to each study, one 10 ml tube was thawed at room temperature for approximately 1 h and then centrifuged for 10 mins at 4700 rpm and  $21^\circ\text{C}$ . The centrifuging caused the bacteria to collect in a pellet at the bottom of the tube and the remaining glycerol solution was jettisoned. The pellet was resuspended in 5 ml of nutrient broth media (Oxoid, referred to as NBM) which had been warmed in a  $37^\circ\text{C}$  water bath. Next, 35 ml of additional NBM, warmed in a  $37^\circ\text{C}$  water bath, was added to the bacteria solution. This mixture was stored overnight in a  $37^\circ\text{C}$  incubator on a shaker plate set to low. The cultures were incubated until the optical density (OD) at 600 nm was approximately 1. The cultures were then further diluted with warm NBM until the OD at 600 nm was approximately 0.35.

### 2.4 Bacteria Adhesion on Different Surfaces

Fluorescence microscopy was used to quantify the number of bacteria that adhered to the surface. Sterilized Ti, NT, NT-S1, and NT-S2 were placed in 24-well plates. 1 ml of the prepared bacterial culture was added to each well. The well plates were placed in a sterile plastic bag and stored in a  $37^\circ\text{C}$  incubator for 6 and 24 h periods. [6] After the incubation period was complete, the NBM was removed from each well and the surfaces were rinsed three times with sterile phosphate buffer solution (PBS). The surfaces were then moved to a clean 48-well plate. The fluorescence stain mixture was prepared by adding  $3\ \mu\text{l}$  of propidium iodide (Fisher Scientific, referred to as PI) and  $3\ \mu\text{l}$  of Syto 9 stain (Fisher Scientific) per 1 ml of sodium chloride solution. [6]  $300\ \mu\text{l}$  of the stain solution was added to each well with the surfaces. The well plates were incubated for 20 mins at  $37^\circ\text{C}$ , at which point the stain solution was removed and the surfaces were washed once more with PBS. [6] The surfaces were then imaged with a Zeiss Axiovision fluorescence microscope. ImageJ was used to calculate the number of live and dead bacteria on different surfaces.

### 2.5 Bacteria Morphology and Biofilm Formation

SEM microscopy was used to investigate the morphology of the adhered bacteria on different surfaces. As with the fluorescence studies, sterilized Ti, NT, NT-S1, and NT-S2 were placed in 24-well plates. 1 ml of the prepared bacterial culture was added to each well. The well plates were placed in a sterile plastic bag and stored in a  $37^\circ\text{C}$  incubator for 6 and 24 h periods. [6] The adhered bacteria were fixed using a process described elsewhere. [40,41] In brief, the surfaces were soaked in a primary fixative made of 0.1 M sucrose, 0.1 M sodium cacodylate, and 3% glutaraldehyde (v/v) in DI water for 45 mins. The surfaces were then moved to the secondary fixative composed of 0.1 M sucrose and 0.1 M sodium cacodylate in DI water. They were kept in this fixative for 12 h overnight. Next a series of ethanol baths – 35%, 50%, 70%, 95%, and 100% ethanol (v/v in DI water) – were used to

dehydrate the surfaces. They were soaked in each bath for 10 mins. They were then moved to a sterile 24-well plate and stored in a desiccator until imaging. They were coated with 10 nm of gold and imaged using SEM at 2 kV.

## 2.6 Statistical Analysis

Surface characterization was reconfirmed on 2 different samples of each surfaces. SEM images and contact angle measurements were taken for at least 6 samples of each surface ( $n_{min} = 6$ ). The fluorescence microscopy was repeated three times for each bacteria type and each time period on at least three surfaces ( $n_{min} = 9$ ). The bacteria morphology studies were repeated three times for each bacteria type and each time period on three substrates each, with at least five images per sample ( $n_{min} = 45$ ). The quantitative results were analyzed using one-way and two-way ANOVA tests as appropriate and the results were considered statistically significant with a p-value  $< 0.05$ .

## 3. Results and Discussion

Preventing bacterial infections are a challenge for many implantable medical devices. Bacterial infections on implant surfaces are characterized by the formation of a biofilm which protects the bacterial colony living on the material surface. The formation of biofilms on an implant's surface starts with bacterial adhesion and so current research is focused on the initial stage of bacterial adhesion and biofilm formation. In this study, we have investigated the ability of superhydrophobic titania nanotube arrays to prevent initial gram-positive and gram-negative bacterial adhesion and further biofilm formation and have compared the results with superhydrophilic and control (unmodified Ti) surfaces.

### 3.1 Surface Characterization

SEM was used to characterize the surface morphology of the titania nanotube arrays. The titania nanotube arrays had an average inner diameter of 150 nm, were vertically oriented, had typical lengths between 1.2 and 1.3  $\mu\text{m}$ , and were uniformly distributed across the surface (Figure 1(a) and 1(b)). After modification with S1 and S2, the average inner diameter of the nanotubes decreased to 140 nm ( $p < 0.05$ ) and 147 nm ( $p < 0.05$ ) respectively (Figure 1(b)). As expected, the orientation and distribution of the modified nanotube arrays remained unchanged (Figure 1(a)). The average wall thickness of the nanotube arrays also increased from 27 nm (NT) after modification to 33 nm (NT-S2) ( $p < 0.05$ ) and 38 nm (NT-S1) ( $p < 0.05$ ). This change was expected due to silanization.

Contact angle goniometry was used to characterize the wettability of different surfaces. The results indicate static, advancing and receding contact angles of 74°, 86°, 41° for Ti, 23°, 31°, 12° for NT, 164°, 166°, 163° for NT-S1, and  $< 5^\circ$ , 7°,  $< 5^\circ$  for NT-S2 (Figure 2). The contact angles for all the surfaces were significantly different from each other ( $p < 0.05$ ). Due to the low contact angle hysteresis (i.e., the difference between advancing and receding contact angles) of NT-S1, droplets of water could easily roll off from such surfaces. The roll-off angle for NT-S1 was 3°, while water did not roll off from the Ti, NT and NT-S2 surfaces. NT-S1 can be considered superhydrophobic as it displays water contact angles greater than 150° and roll-off angle under 10°. The solid surface energies were determined to be



approximately 40 mN/m for Ti and NT, 11 mN/m for NT-S1, and 50 mN/m for NT-S2 through Owens-Wendt analysis, which are consistent with previously published data on titania nanotube arrays.[15,37,40]

A droplet on a textured surface will enter either the Wenzel state [42] or the Cassie–Baxter state.[43] The Wenzel state is where the droplet penetrates the surface asperities, completely wetting the surface.[44,45] This state is expected for NT and NT-S2. The Cassie–Baxter state is when air pockets remain trapped within the texture, leading to the droplet being partly suspended above the surface. The Cassie–Baxter state is preferred for obtaining high contact angles and low contact angles hysteresis. This is because of the reduced contact area between the droplet and the surface, which in turn is due to the presence of the air pockets. [44,45] This state is expected for NT-S1. It is expected that by minimizing the contact area between the liquid and a surface, bacterial adhesion and biofilm formation can be reduced.

XPS was used to determine the relative compositions of elements on the different surfaces to characterize their surface chemistry. O1s, Ti2p<sub>3/2</sub>, and C1s peaks were present on all surfaces (Figure 3). The NT surfaces showed a lower C1s peak than Ti because the anodization and etching process removes some of the carbon naturally present on the surface (some carbon is due to the contamination of the XPS chamber). The NT-S1 and NT-S2 both have C1s peaks because the silanes which bonded to the surface of titania nanotube arrays contain carbon. The NT-S1 surfaces also had a large F1s peak (along with a CF<sub>2</sub> and CF<sub>3</sub> peaks in high resolution scans due to the use of fluorinated silane, data not shown). The F1s peak was absent on the other surfaces. Additionally, Si1s peaks were present on both NT-S1 and NT-S2 since both the silanes contain silicon. The results are consistent with previously published XPS spectra for Ti, NT and NT-S1 since they were fabricated in similar way.[31] The presence of these peaks confirms that the titania nanotube arrays were successfully modified by silanes.

X-ray diffraction was used to characterize the presence of different crystal structures of titania (Ti  $\alpha$ , anatase and rutile) on the different surfaces. The XRD scans show anatase and Ti  $\alpha$  phases, along with a small rutile phase (Figure 4). The crystal phases for the nanotube arrays differ from titanium, indicating that the fabrication process changed the underlying crystal structures of the titania nanotube arrays.[31,32] The phases do not differ between the different nanotube arrays, however, indicating that the silanization process does not affect the underlying crystal structure.[31,32] These results are also consistent with previously published XRD spectra for titania nanotube arrays.[31]

### 3.2 Bacteria Adhesion and Biofilm Formation

Fluorescence microscopy was used to investigate the adhesion of *S. aureus* and *P. aeruginosa* bacteria to different surfaces. Two different stains, Syto-9 and PI, were used to stain the bacteria on different surfaces. The Syto-9 stain is able to penetrate the cell walls of living bacteria while the PI stain is not, meaning that living bacteria will appear green under a fluorescence microscope.[6] The PI stain is able to attach to dead bacteria and is commonly used to identify dead cells, which will appear red under a fluorescence microscope after staining.[6] The use of these two stains enables the simultaneous imaging of living and dead bacteria on the test surfaces.

The results for *S. aureus* indicated that the adhesion of live (green) and dead (red) bacteria was highest on Ti after 6 h and 24 h of culture as compared to all other surfaces (Figure 5 (a) and (b)) ( $p < 0.05$ ). This was followed by lower adhesion on NT and NT-S2 surfaces ( $p < 0.05$ ). Further, NT-S1 showed the least adhesion of *S. aureus* compared to all other surfaces after 6 and 24 h of culture (Figure 5(a) and (b)) ( $p < 0.05$ ). Similar results were observed with *P. aeruginosa*. The results indicated that the adhesion of live (green) and dead (red) bacteria was highest on Ti after both 6 h and 24 h (Figure 6(a) and (b)) ( $p < 0.05$ ). The NT and NT-S2 surfaces showed less adhesion than Ti, while the NT-S1 surface showed the least adhesion of *P. aeruginosa* compared to all other surfaces after 6 and 24 h of culture (Figure 6(a) and (b)) ( $p < 0.05$ ). These results indicate that Ti and NT-S1 behaved as expected, with Ti having the highest bacterial adhesion and the superhydrophobic NT-S1 having the lowest bacterial adhesion. The NT (hydrophilic) and NT-S2 (superhydrophilic) showed reduced bacterial adhesion compared to Ti, which is also consistent with previous studies on titania nanotube arrays.[11,46] The differences in bacterial adhesion between the NT and NT-S2 surfaces were not statistically significant. Previous studies have shown that bacteria are easier to remove from superhydrophobic surfaces.[18] These studies have suggested that the reduced surface energy of the superhydrophobic surfaces along with their tendency to reduce protein adsorption to the surface makes it more difficult for bacteria to adhere, reducing adhesion and making it easier to remove those that do attach.[15,18,47] In this work, silanization with the fluorinated silane reduced the surface energy of the NT-S1. For this reason, the reduction in bacteria adhesion on the NT-S1 was expected. Conversely, the silanization with the methoxysilane did not significantly change the surface energy of the NT-S2 compared to the NT, and hence did not have significantly different bacterial adhesion.

### 3.3 Bacteria Morphology and Biofilm Formation

SEM was used to investigate the morphology of *S. aureus* and *P. aeruginosa* on different surfaces. Bacteria are expected to colonize and form biofilms on most material surfaces. The results for *S. aureus* showed more attached bacteria on all surfaces after 24 h as compared to 6 h (Figure 7(a)). This was expected as the longer incubation period allowed more time for the bacterial colonies to develop and form.[6,17] Consistent with the fluorescence microscopy results, the Ti had the most adhered bacteria. After 24 h, large colonies formed across the Ti surface with some initial biofilm formation as seen in the SEM images (Figures 7(a) and 7(b)). The other surfaces showed no biofilm formation, with some colony formation evident on the NT after 24 h. The *S. aureus* remained mostly in small groups and showed little aggregation on the NT-S1 and NT-S2 samples. The *P. aeruginosa* results were also similar to the fluorescence microscopy results. No surfaces showed significant colony formation after 6 h, as the bacteria did not aggregate on any surface (Figure 7(b)). However, after 24 h on Ti, the bacteria had nearly covered the surfaces and formed biofilms. The NT-S2 showed some colony formation after 24 h. On the NT and NT-S1 samples, the adhered bacteria were still mostly individual cells with little aggregation after 24 h. The SEM results also show the impact of flaws in the titania nanotube arrays, as bacteria can be seen adhered within the grooves or in the spaces between nanotube arrays. The NT-S1 surfaces that were fabricated to be superhydrophobic with the fluorinated silane showed reduced bacterial adhesion in the SEM images and fluorescence microscopy. However, the NT-S2 surfaces that were fabricated to be superhydrophilic with methoxysilane did not significantly change



bacterial adhesion compared to the NT surfaces. These results indicate that both the nanostructure and superhydrophobic surface chemistry contributes to reduced bacterial adhesion.

#### 4. Conclusion

Combating bacterial infections is a challenge for patients who receive an implanted medical device. Reducing the occurrence of bacterial infections is important in order to reduce device failure and improve patients' quality of life. Due to the increase in antibiotic-resistant bacteria strains, new approaches that do not create bacterial resistance are necessary for infection rates to be reduced. Titania nanotube arrays have shown some ability to reduce bacterial adhesion, but there is little research on how superhydrophobic surfaces affect bacterial adhesion. In this work, we have fabricated superhydrophobic and superhydrophilic titania nanotube arrays by anodizing and chemically etching titanium and then modifying the surface chemistry through silanization. The adhesion of gram-positive *S. aureus* and gram-negative *P. aeruginosa* bacteria was investigated by incubating the substrates in bacteria solutions for 6 h and 24 h. The number of adhered bacteria were calculated from fluorescence microscopy images using propidium iodide and Syto-9 stains to distinguish between dead and living bacteria respectively. The results showed fewer bacteria adhered to the superhydrophobic surfaces than any other surface, while the superhydrophilic surfaces were not significantly better than unmodified titania nanotube arrays in reducing the adhesion of bacteria. It is important to note that the superhydrophobic surfaces had minimal bacteria attached after 24 h and did not repel bacteria completely. However, no biofilm formation was observed. Future work will investigate the attachment of bacteria beyond 24 h, the long-term durability of superhydrophobic coatings on nanotube arrays, and the ways in which superhydrophobicity can be enhanced. Future investigations will also examine the adsorption of proteins involved in bacterial attachment on superhydrophobic surfaces. Additionally, other strains of bacteria, including bacteria which do not fall into the traditional gram staining categories, will be investigated.

#### Acknowledgments

Research reported in this was supported by *National Heart, Lung and Blood Institute* of the National Institutes of Health under award number R01HL135505. The content is solely the responsibility of the authors and does not necessarily represent the official views of the National Institutes of Health.

#### References

1. Darouiche RO. Device-associated infections: a macroproblem that starts with microadherence. *Clin. Infect. Dis.* 2001; 33:1567–1572. DOI: 10.1086/323130 [PubMed: 11577378]
2. Sandoe JAT, Witherden IR, Cove JH, Heritage J, Wilcox MH. Correlation between enterococcal biofilm formation in vitro and medical-device-related infection potential in vivo. *J. Med. Microbiol.* 2003; 52:547–550. DOI: 10.1099/jmm.0.05201-0 [PubMed: 12808074]
3. Zago CE, Silva S, Sanitá PV, Barbugli PA, Dias CMI, Lordello VB, Vergani CE. Dynamics of biofilm formation and the Interaction between *Candida albicans* and methicillin-susceptible (MSSA) and -resistant *Staphylococcus aureus* (MRSA). *PLoS One.* 2015; 10:1–15. DOI: 10.1371/journal.pone.0123206
4. Costerton JW. Bacterial Biofilms: A Common Cause of Persistent Infections. *Science (80-.)*. 1999; 284:1318–1322. DOI: 10.1126/science.284.5418.1318

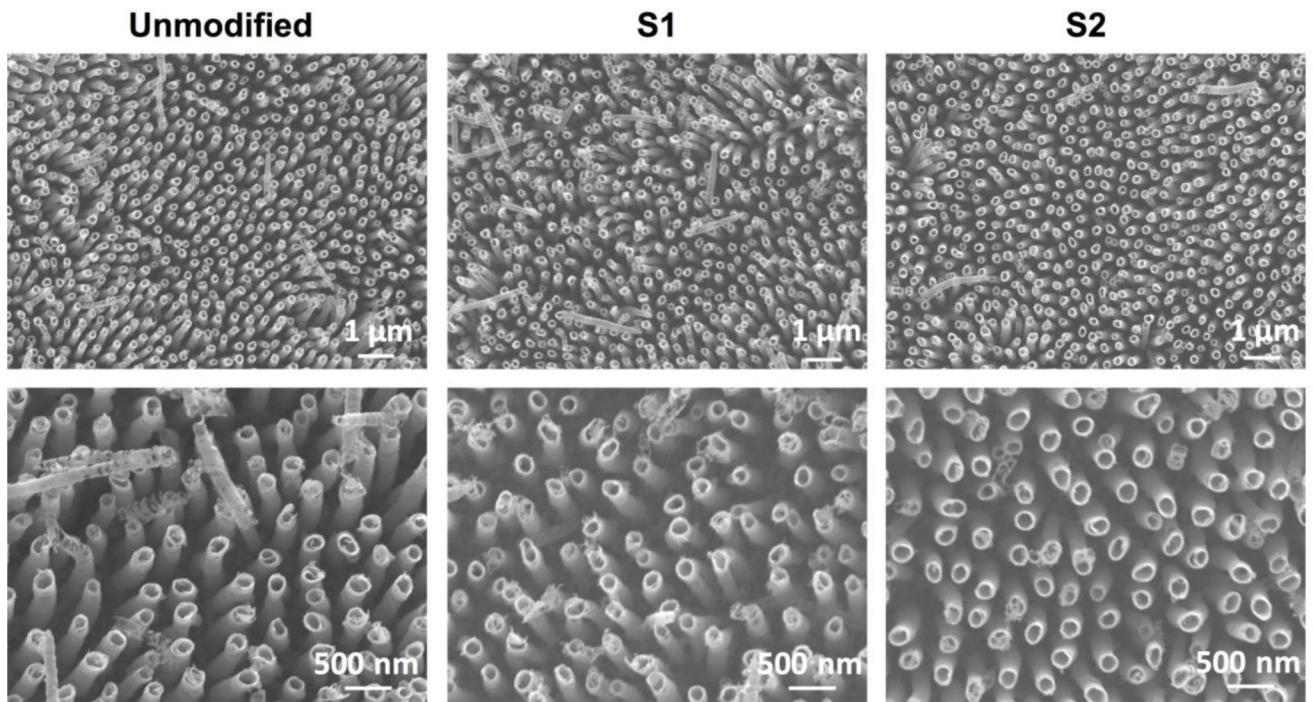
5. Hori K, Matsumoto S. Bacterial adhesion: From mechanism to control. *Biochem. Eng. J.* 2010; 48:424–434. DOI: 10.1016/j.bej.2009.11.014
6. Neufeld BH, Reynolds MM. Critical nitric oxide concentration for *Pseudomonas aeruginosa* biofilm reduction on polyurethane substrates. *Biointerphases.* 2016; 1111:31012.doi: 10.1116/1.4962266
7. Sousa C, Rodrigues D, Oliveira R, Song W, Mano JF, Azeredo J. Superhydrophobic poly(L-lactic acid) surface as potential bacterial colonization substrate. *AMB Express.* 2011; 1:34.doi: 10.1186/2191-0855-1-34 [PubMed: 22018163]
8. Kiremitci-Gumusderelioglu M, Pesmen A. Microbial adhesion to ionogenic PHEMA, PU and PP implants. *Biomaterials.* 1996; 17:443–449. DOI: 10.1016/0142-9612(96)89662-1 [PubMed: 8938240]
9. Speranza G, Gottardi G, Pederzoli C, Lunelli L, Canteri R, Pasquardini L, Carli E, Lui A, Maniglio D, Brugnara M, Anderle M. Role of chemical interactions in bacterial adhesion to polymer surfaces. *Biomaterials.* 2004; 25:2029–2037. DOI: 10.1016/j.biomaterials.2003.08.061 [PubMed: 14741617]
10. Zhang X, Shi F, Niu J, Jiang Y, Wang Z. Superhydrophobic surfaces: from structural control to functional application. *J. Mater. Chem.* 2008; 18:621–633. DOI: 10.1039/b711226b
11. Banerjee I, Pangule RC, Kane RS. Antifouling coatings: Recent developments in the design of surfaces that prevent fouling by proteins, bacteria, and marine organisms. *Adv. Mater.* 2011; 23:690–718. DOI: 10.1002/adma.201001215 [PubMed: 20886559]
12. Poortinga AT, Bos R, Norde W, Busscher HJ. Electric double layer interactions in bacterial adhesion to surfaces. 2002; doi: 10.1016/S0167-5729(02)00032-8
13. Abe S, Ishihara K, Okuda K. Prevalence of potential respiratory pathogens in the mouths of elderly patients and effects of professional oral care. *Arch. Gerontol. Geriatr.* 2001; 32:45–55. DOI: 10.1016/S0167-4943(00)00091-1 [PubMed: 11251238]
14. Harris LG, Tosatti S, Wieland M, Textor M, Richards RG. *Staphylococcus aureus* adhesion to titanium oxide surfaces coated with non-functionalized and peptide-functionalized poly(L-lysine)-grafted- poly(ethylene glycol) copolymers. *Biomaterials.* 2004; 25:4135–4148. DOI: 10.1016/j.biomaterials.2003.11.033 [PubMed: 15046904]
15. Lin C, Tang P, Zhang W, Wang Y, Zhang B, Wang H, Zhang L. Effect of superhydrophobic surface of titanium on *staphylococcus aureus* adhesion. *J. Nanomater.* 2011; 2011doi: 10.1155/2011/178921
16. Dong H, Zeng G, Tang L, Fan C, Zhang C, He X, He Y. An overview on limitations of TiO<sub>2</sub>-based particles for photocatalytic degradation of organic pollutants and the corresponding countermeasures. *Water Res.* 2015; 79:128–146. DOI: 10.1016/j.watres.2015.04.038 [PubMed: 25980914]
17. Fadeeva E, Truong VK, Stiesch M, Chichkov BN, Crawford RJ, Wang J, Ivanova EP. Bacterial retention on superhydrophobic titanium surfaces fabricated by femtosecond laser ablation. *Langmuir.* 2011; 27:3012–3019. DOI: 10.1021/la104607g [PubMed: 21288031]
18. Zhang X, Wang L, Levänen E. Superhydrophobic surfaces for the reduction of bacterial adhesion. *RSC Adv.* 2013; 3:12003.doi: 10.1039/c3ra40497h
19. Barthlott W, Neinhuis C. Purity of the sacred lotus, or escape from contamination in biological surfaces. *Planta.* 1997; 202:1–8. DOI: 10.1007/s004250050096
20. Bandara CD, Singh S, Afara IO, Tesfamichael T, Wolff A, (Ken) Ostrikov K, Oloyede A. Bactericidal Effects of Natural Nanotopography of Dragonfly Wing on *Escherichia coli*. *ACS Appl. Mater. Interfaces.* 2017; acsami.6b13666. doi: 10.1021/acsami.6b13666
21. Ma J, Sun Y, Gleichauf K, Lou J, Li Q. Nanostructure on taro leaves resists fouling by colloids and bacteria under submerged conditions. *Langmuir.* 2011; 27:10035–10040. DOI: 10.1021/la2010024 [PubMed: 21736298]
22. Mahalakshmi PV, Vanithakumari SC, Gopal J, Mudali UK, Raj B. Enhancing corrosion and biofouling resistance through superhydrophobic surface modification. *Curr. Sci.* 2011; 101:1328–1336.
23. Nosonovsky M, Bhushan B. Superhydrophobic surfaces and emerging applications: Non-adhesion, energy, green engineering. *Curr. Opin. Colloid Interface Sci.* 2009; 14:270–280. DOI: 10.1016/j.cocis.2009.05.004

24. Movafaghi S, Wang W, Metzger A, Williams DD, Williams JD, Kota AK. Tunable superomniphobic surfaces for sorting droplets by surface tension. *Lab Chip*. 2016; 16:3204–3209. DOI: 10.1039/C6LC00673F [PubMed: 27412084]
25. Li L, Tian J, Li M, Shen W. Superhydrophobic surface supported bioassay - An application in blood typing. *Colloids Surfaces B Biointerfaces*. 2013; 106:176–180. DOI: 10.1016/j.colsurfb.2013.01.049 [PubMed: 23434709]
26. Gentile F, Coluccio ML, Coppede N, Mecarini F, Das G, Liberale C, Tirinato L, Leoncini M, Perozziello G, Candeloro P, De Angelis F, Di Fabrizio E. Superhydrophobic surfaces as smart platforms for the analysis of diluted biological solutions. *ACS Appl. Mater. Interfaces*. 2012; 4:3213–3224. DOI: 10.1021/am300556w [PubMed: 22620470]
27. Zhang D, Li G, Wang H, Chan KM, Yu JC. Biocompatible anatase single-crystal photocatalysts with tunable percentage of reactive facets. *Cryst. Growth Des*. 2010; 10:1130–1137. DOI: 10.1021/cg900961k
28. Gottenbos B, Van Der Mei HC, Busscher HJ, Grijpma DW, Feijen J. Initial adhesion and surface growth of *Pseudomonas aeruginosa* on negatively and positively charged poly(methacrylates). *J. Mater. Sci. Mater. Med*. 1999; 10:853–855. DOI: 10.1023/A:1008989416939 [PubMed: 15347964]
29. a Jucker B, a Jucker B, Harms H, Harms H, Zehnder AJB, Zehnder AJB. Adhesion of the Positively Charged Bacterium. *Microbiology*. 1996; 178:5472–5479.
30. Nonkreman CJ, Fleith S, Rouxhet PG, Dupont-Gillain CC. Competitive adsorption of fibrinogen and albumin and blood platelet adhesion on surfaces modified with nanoparticles and/or PEO. *Colloids Surfaces B Biointerfaces*. 2010; 77:139–149. DOI: 10.1016/j.colsurfb.2010.01.014 [PubMed: 20171850]
31. Bartlett K, Movafaghi S, Kota A, Popat KC. Superhemophobic titania nanotube array surfaces for blood contacting medical devices. *RSC Adv*. 2017; 7:35466–35476. DOI: 10.1039/C7RA03373G
32. Sorkin JA, Hughes S, Soares P, Popat KC. Titania nanotube arrays as interfaces for neural prostheses. *Mater. Sci. Eng. C*. 2015; 49:735–745. DOI: 10.1016/j.msec.2015.01.077
33. Smith BS, Yoriya S, Johnson T, Popat KC. Dermal fibroblast and epidermal keratinocyte functionality on titania nanotube arrays. *Acta Biomater*. 2011; 7:2686–2696. DOI: 10.1016/j.actbio.2011.03.014 [PubMed: 21414425]
34. Smith BS, Capellato P, Kelley S, Gonzalez-Juarrero M, Popat KC. Reduced in vitro immune response on titania nanotube arrays compared to titanium surface. *Biomater. Sci*. 2013; 1:322–332. DOI: 10.1039/c2bm00079b
35. Capellato P, Escada AL, Popat KC, Claro AP. Interaction between mesenchymal stem cells and Ti-30Ta alloy after surface treatment. *J Biomed Mater Res A*. 2013; :2147–2156. DOI: 10.1002/jbm.a.34891 [PubMed: 23893959]
36. Capellato P, Smith BS, Popat KC, Claro AP. Fibroblast functionality on novel Ti30Ta nanotube array. *Mater. Sci. Eng. C*. 2012; 32:2060–2067. DOI: 10.1016/j.msec.2012.05.013
37. Kota AK, Li Y, Mabry JM, Tuteja A. Hierarchically structured superoleophobic surfaces with ultralow contact angle hysteresis. *Adv. Mater*. 2012; 24:5838–5843. DOI: 10.1002/adma.201202554 [PubMed: 22930526]
38. Riedel NA, Smith BS, Williams JD, Popat KC. Improved thrombogenicity on oxygen etched Ti6Al4V surfaces. *Mater. Sci. Eng. C*. 2012; 32:1196–1203. DOI: 10.1016/j.msec.2012.03.008
39. Owens DK, De Nemours EIP, Film S. Estimation of the Surface Free Energy of Polymers. *J. Appl. Polym. Sci*. 1969; 13:1741–1747.
40. Movafaghi S, Leszczak V, Wang W, Sorkin JA, Dasi LP, Popat KC, Kota AK. Hemocompatibility of Superhemophobic Titania Surfaces. *Adv. Healthc. Mater*. 2016; :1600717.doi: 10.1002/adhm.201600717
41. Smith BS, Yoriya S, Grissom L, Grimes CA, Popat KC. Hemocompatibility of titania nanotube arrays. *J. Biomed. Mater. Res. - Part A*. 2010; 95 A:350–360. DOI: 10.1002/jbm.a.32853
42. Wenzel RN. Resistance of solid surfaces to wetting by water. *Ind. Eng. Chem*. 1936; 28:988–994. DOI: 10.1021/ie50320a024
43. Cassie ABD, Baxter S. Wettability of porous surfaces. *Trans. Faraday Soc*. 1944; 40:546.doi: 10.1039/TF9444000546

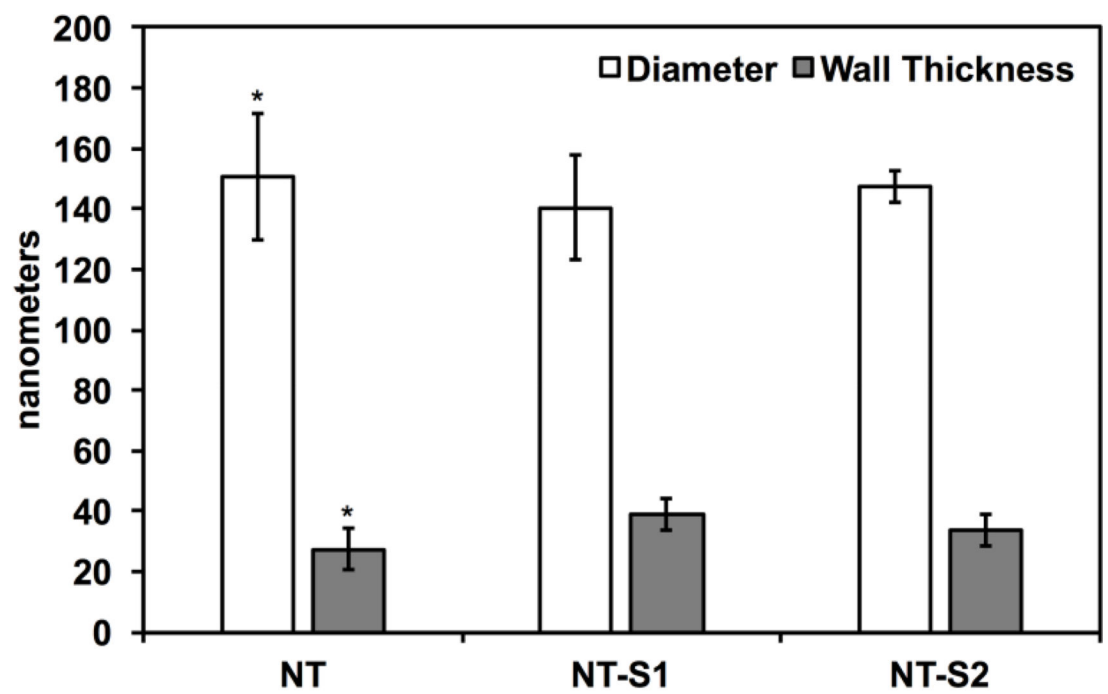
44. Lafuma A, Quéré D. Superhydrophobic states. *Nat. Mater.* 2003; 2:457–460. DOI: 10.1038/nmat924 [PubMed: 12819775]
45. Wang W, Lockwood K, Boyd LM, Davidson MD, Movafaghi S, Vahabi H, Khetani SR, Kota AK. Superhydrophobic Coatings with Edible Materials. *ACS Appl. Mater. Interfaces.* 2016; 8:18664–18668. DOI: 10.1021/acsami.6b06958 [PubMed: 27403590]
46. Trujillo NA, Oldinski RA, Ma H, Bryers JD, Williams JD, Popat KC. Antibacterial effects of silver-doped hydroxyapatite thin films sputter deposited on titanium. *Mater. Sci. Eng. C.* 2012; 32:2135–2144. DOI: 10.1016/j.msec.2012.05.012
47. Zhu H, Guo Z, Liu W. Adhesion behaviors on superhydrophobic surfaces. *Chem. Commun.* 2014; 50:3900.doi: 10.1039/c3cc47818a

### Highlights

- Uniform titania nanotubes arrays can be fabricated using anodization
- Superhydrophobic titania nanotube arrays have contact angles  $> 150^\circ$
- Superhydrophobic titania nanotube arrays reduce bacterial adhesion



(a):



(b):

**Figure 1.**

(a): Representative SEM images of titania nanotube arrays before and after surface modification



**(b):** Average diameter and wall thickness of titania nanotube arrays before and after surface modification. Diameter and wall thickness of the NT was significantly different than that of NT-S1 and NT-S2 ( $p < 0.05$ ). Error bars represent standard deviation.

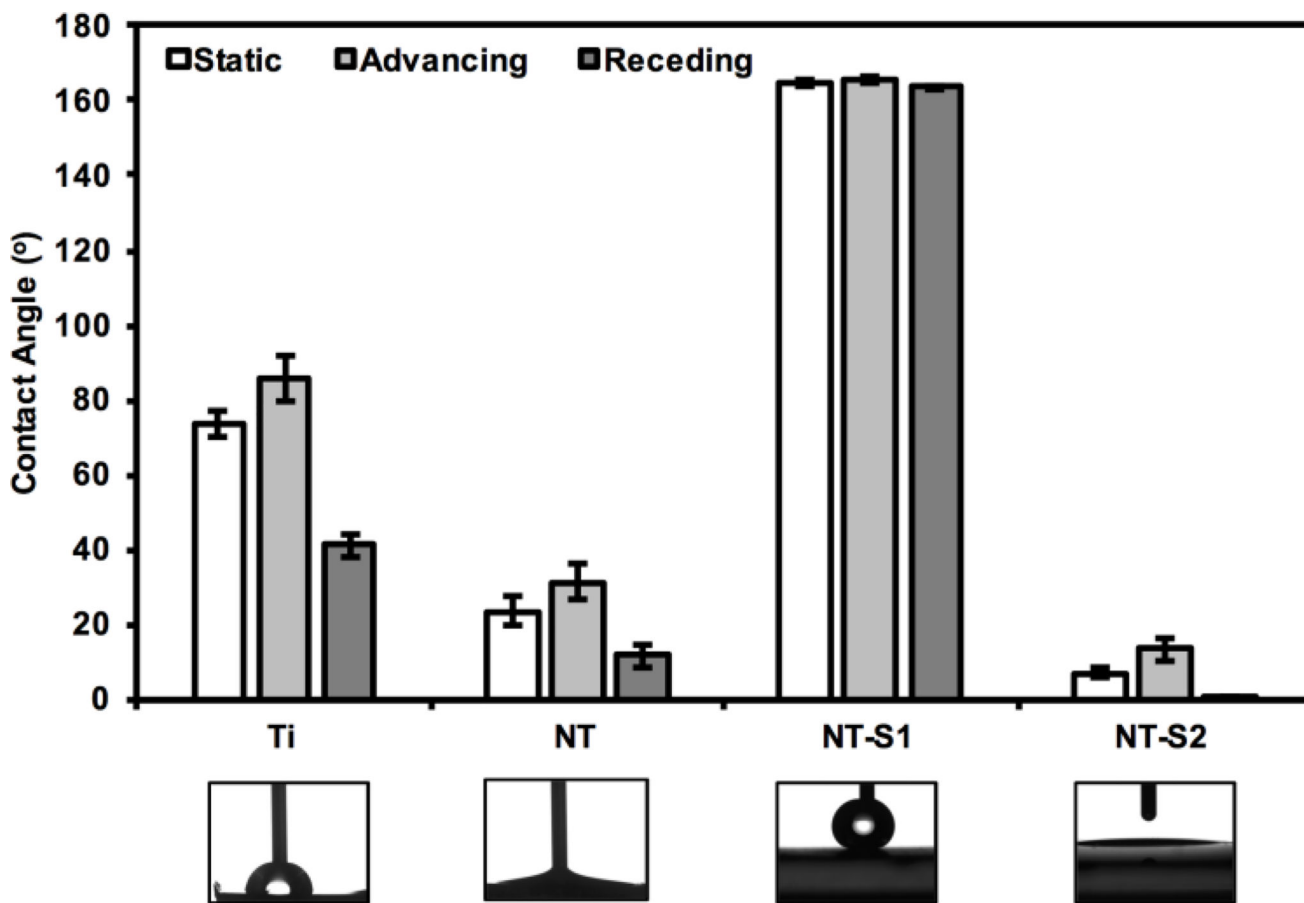


**Figure 2.** Contact angle measurements (static, advancing and receding) for different surfaces along with representative images of water droplet on different surfaces. Note: Statistical symbols are not used in this figure. Contact angles for all surfaces were significantly different from each other ( $p < 0.05$ ). Error bars represent standard deviation.

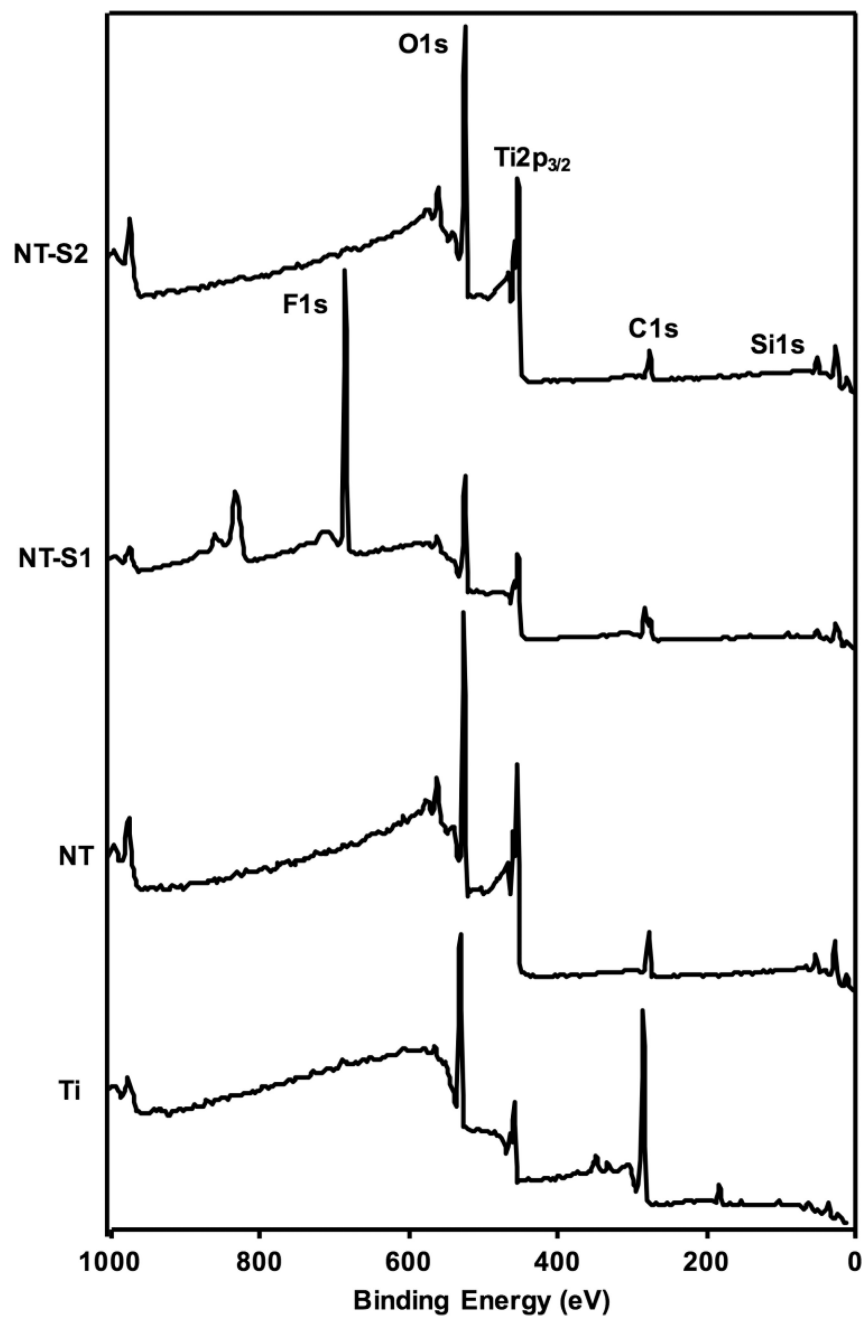


**Figure 3.**  
Representative XPS survey scans for different surfaces.

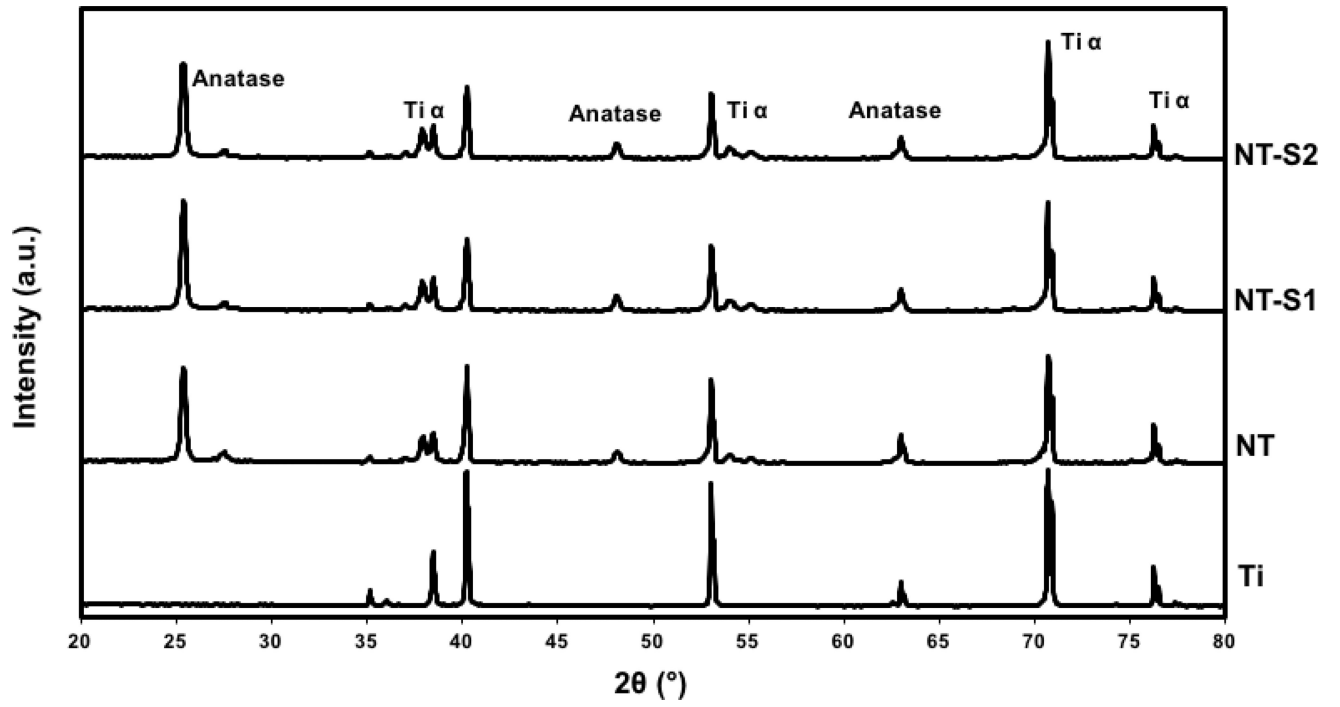
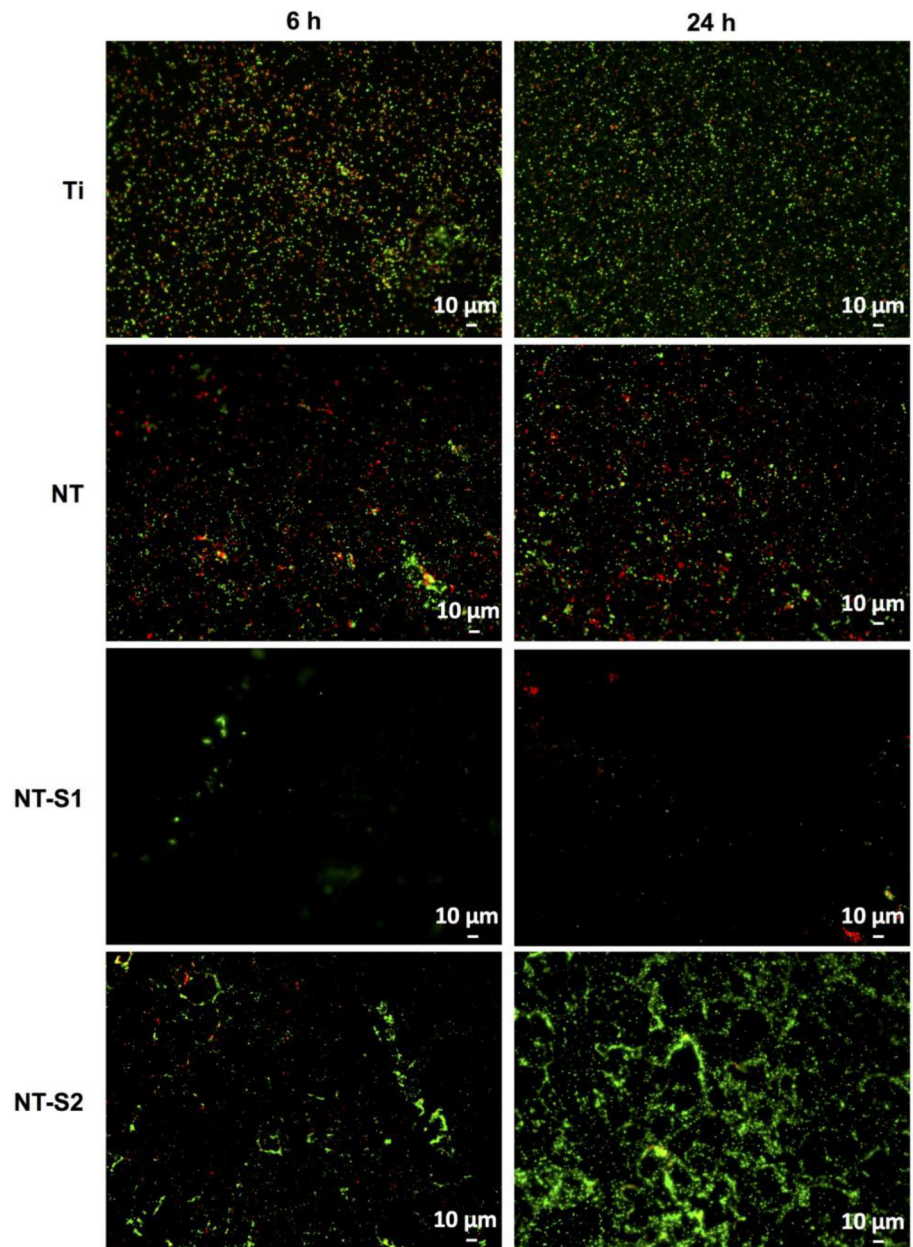
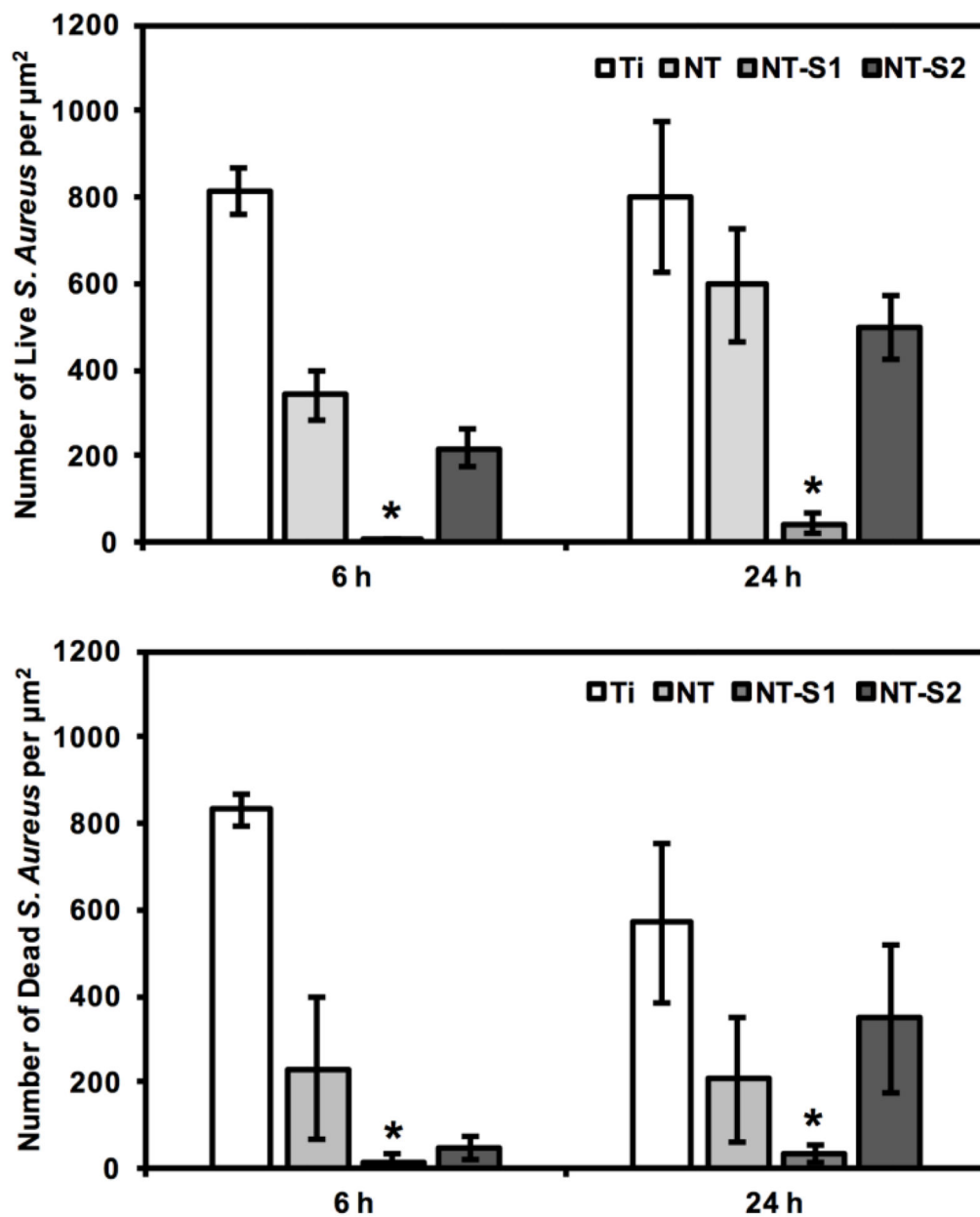


**Figure 4.**  
Representative XRD scans for different surfaces.



(a):



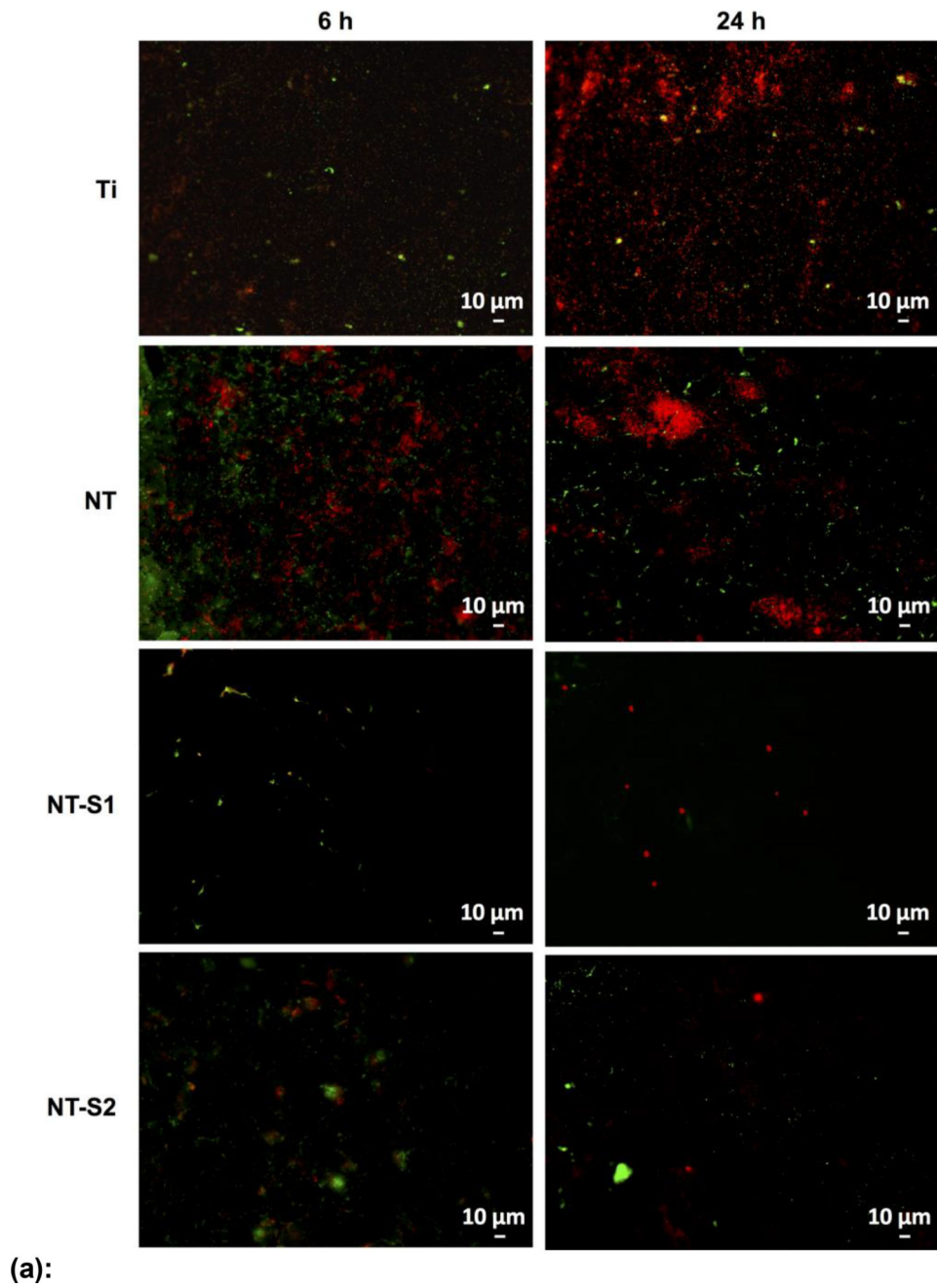
**(b):**

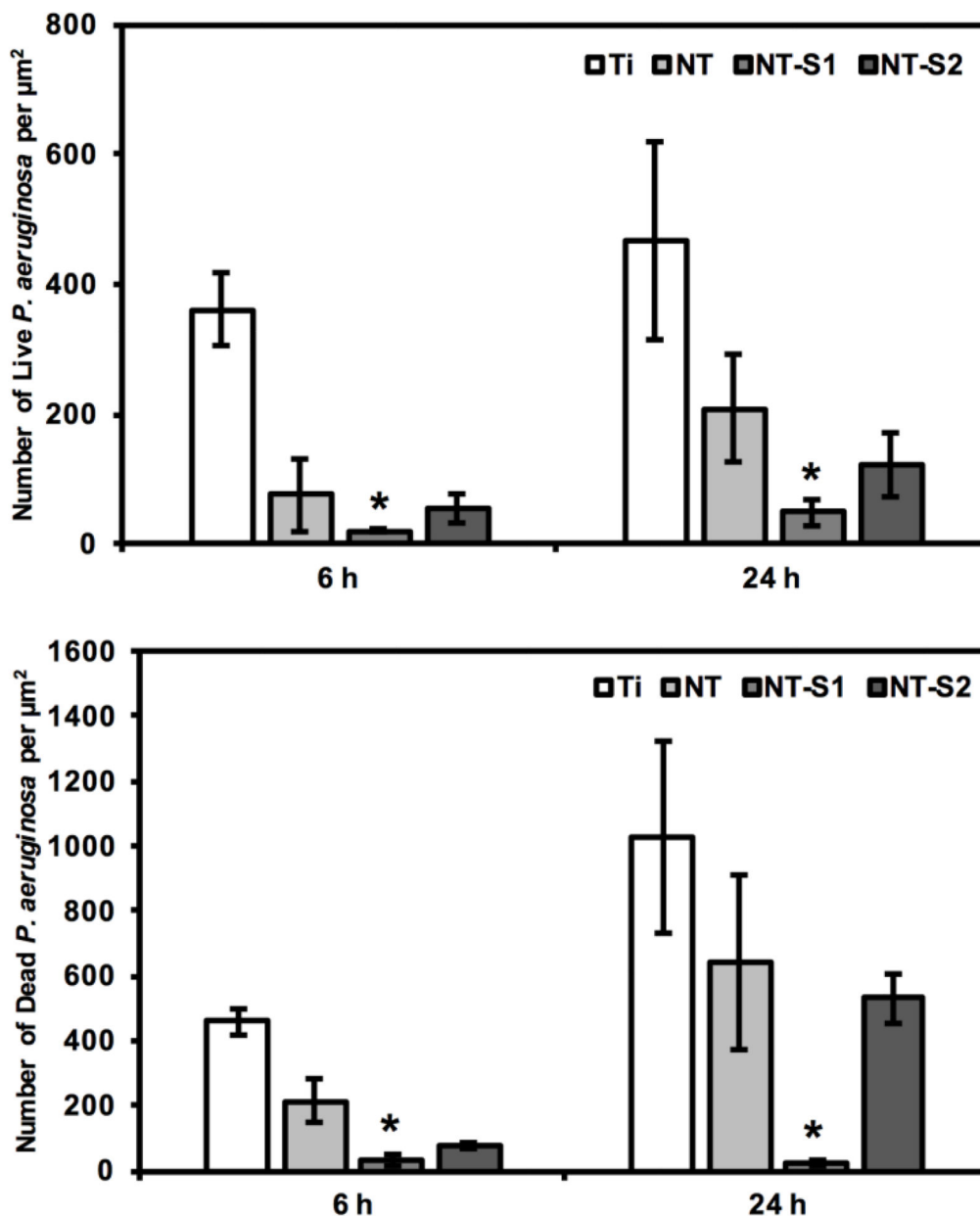
**Figure 5.**

**(a):** Representative fluorescence microscopy images of *S. aureus* on different surfaces after 6 h and 24 h of culture. Green stain represents live bacteria and red stain represents dead bacteria on different surfaces.

**(b):** *S. aureus* adhesion on different surfaces after 6 h and 24 h of culture. Number of adhered bacteria on NT-S1 was significantly lower than that on other surfaces ( $p < 0.05$ ).





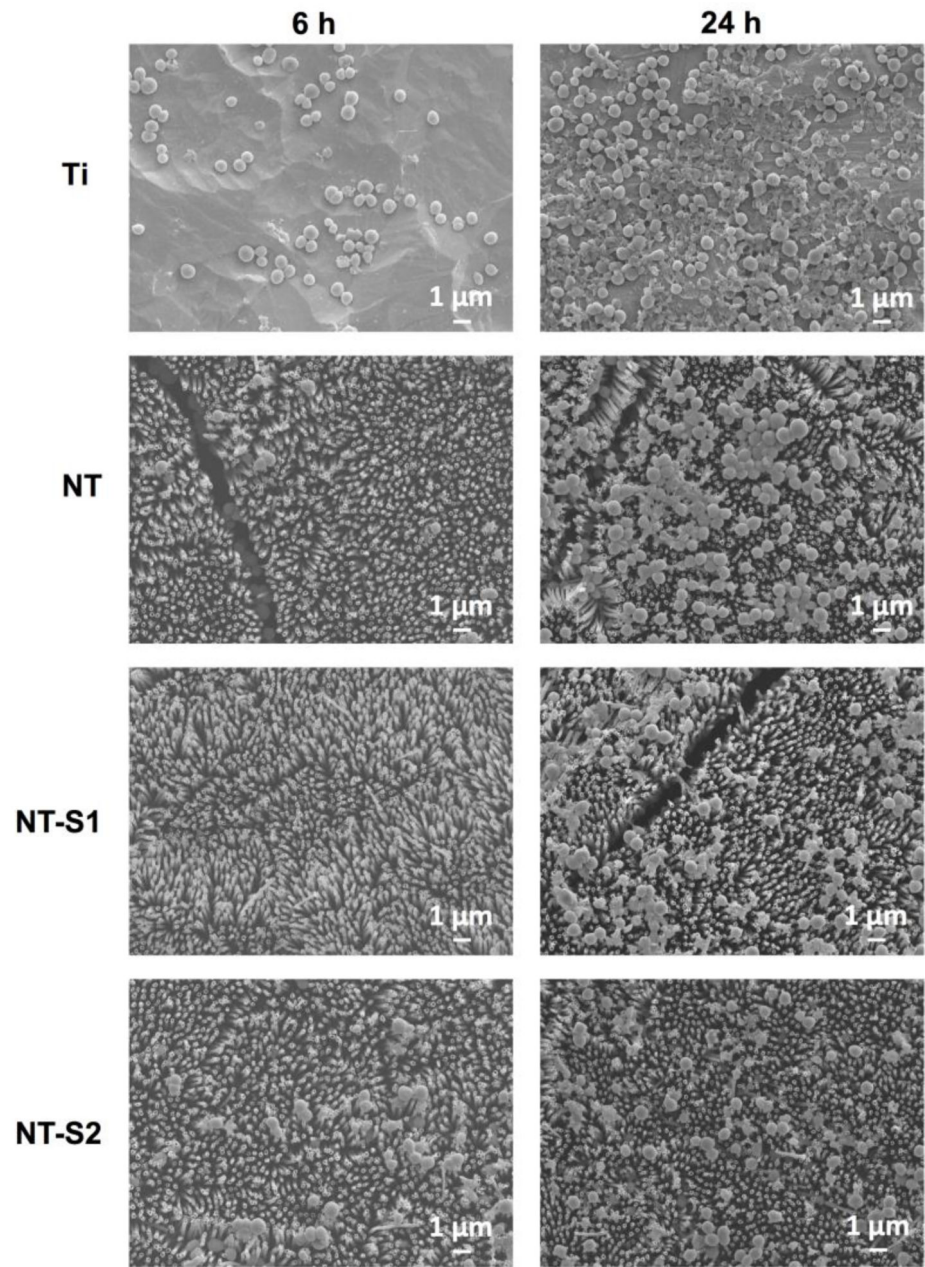


**(b):**

**Figure 6.**

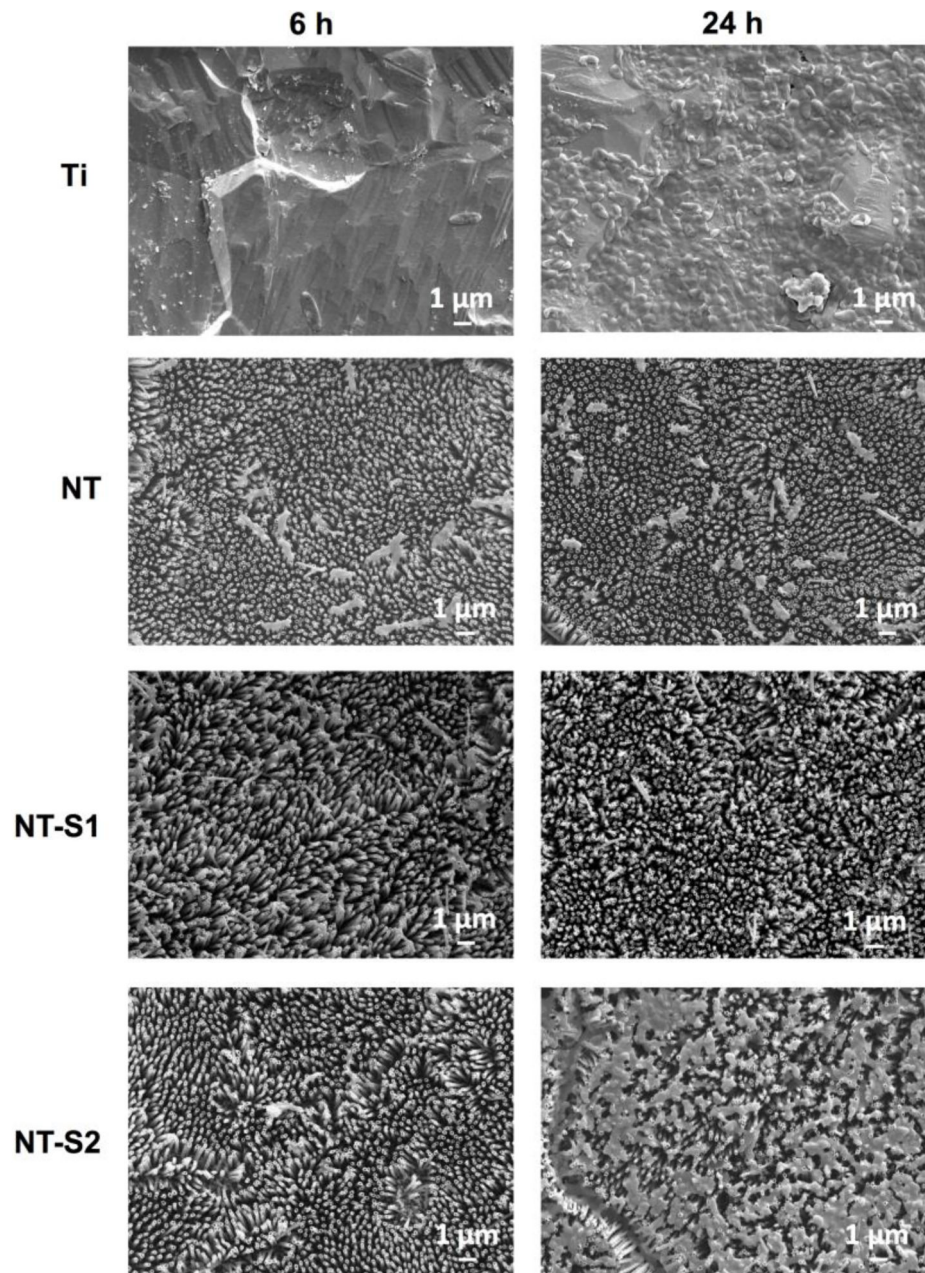
**(a):** Representative fluorescence microscopy images of *P. aeruginosa* on different surfaces after 6 h and 24 h of culture. Green stain represents live bacteria and red stain represents dead bacteria on different surfaces.

**(b):** *P. aeruginosa* adhesion on different surfaces after 6 h and 24 h of culture. Number of adhered bacteria on NT-S1 was significantly lower than that on other surfaces ( $p < 0.05$ ).



(a):





**(b):**

**Figure 7.**

**(a):** Representative SEM images of *S. aureus* on different surfaces.

**(b):** Representative SEM images of *P. aeruginosa* on different surfaces.